

**THE EFFECTS OF CT-BASED ATTENUATION
CORRECTION ON THE ACCURACY OF ^{99m}Tc SPECT/CT
QUANTIFICATION**

SHAMALAH A/P S VIJAYAKUMAR

**SCHOOL OF HEALTH SCIENCES
UNIVERSITI SAINS MALAYSIA**

2024

THE EFFECTS OF CT-BASED ATTENUATION CORRECTION
ON THE ACCURACY OF ^{99m}Tc SPECT/CT QUANTIFICATION

By

SHAMALAH A/P S VIJAYAKUMAR

Dissertation submitted in partial fulfilment of the requirements for the
degree of Bachelor of Health Science (Honours) (Medical Radiation)

AUGUST 2024

CERTIFICATE

This is to certify that the dissertation entitled “**THE EFFECTS OF CT-BASED ATTENUATION CORRECTION ON THE ACCURACY OF ^{99m}Tc SPECT/CT QUANTIFICATION**” is the bona fide record of research work done by **SHAMALAH A/P S VIJAYAKUMAR** during the period from October 2023 to August 2024 under my supervision. I have read this dissertation and that in my opinion it conforms to acceptable standards of scholarly presentation and is fully adequate, in scope and quality, as a dissertation to be submitted in partial fulfilment for the degree of Bachelor of Health Science (Honours) (Medical Radiation).

Supervisor,

Dr. Marianie binti Musaruddin

University Lecturer,

School of Health Sciences Health Campus

Universiti Sains Malaysia,

16150 Kubang Kerian Kelantan, Malaysia

Date: August 2024

Co-supervisor,

Dr. Mohammad Khairul Azhar Abdul

Razab

University Lecturer,

School of Health Sciences Health Campus

Universiti Sains Malaysia,

16150 Kubang Kerian Kelantan, Malaysia

Date: August 2024

DECLARATION

I hereby declare that this dissertation is the result of my own investigations, except where otherwise stated and duly acknowledged. I also declare that it has not been previously or concurrently submitted as a whole for any other degrees at Universiti Sains Malaysia or other institutions. I grant Universiti Sains Malaysia the right to use the dissertation for teaching, research and promotional purposes.

SHAMALAH A/P S VIJAYAKUMAR

Date: August 2024

ACKNOWLEDGEMENT

First and foremost, I want to express my gratitude to the Almighty God for providing me with the opportunity, endurance, and fortitude necessary to successfully finish this dissertation. To start with I would like to sincerely thank Dr. Marianie binti Musaruddin, my supervisor for her crucial guidance, unwavering support and insightful criticism during this research work. Her extensive experience and understanding have been invaluable in helping to shape this dissertation. The quality of this study has been much improved by her meticulous attention to detail and dedication to high standards. I also want to express my gratitude to Dr. Mohammad Khairul Azhar Abdul Razab, my co-supervisor for his wise counsel and support. I would want to express my sincere gratitude for his hard work and willingness to take the time to proofread and edit my work since it enabled me to complete it on time. Without his continuous encouragement to keep working on my dissertation, I could not have finished it in time.

In addition, I would want to use this chance to express my gratitude to my field-supervisor, Encik Muhammad Yusri bin Udin who helped me finish my study by providing support and direction while I conducted my research. He was a big assistance and mentor when it came to carrying out the experiment for the study. He shared his expertise about my research and answered all of my endless inquiries with such patience that I will always be grateful. Moreover, I have the utmost gratitude to my family for their consistent support, tolerance, and comprehension during this academic journey. Their support and affection have been my rock of strength through difficult times. Finally, I would like to thank Universiti Sains Malaysia for its financial assistance and resources, which were essential to the accomplishment of this dissertation.

Table of Contents

CERTIFICATE.....	ii
DECLARATION.....	iii
ACKNOWLEDGEMENT	iv
LIST OF TABLES	viii
LIST OF FIGURES	ix
LIST OF SYMBOLS	x
LIST OF ABBREVIATIONS	xi
ABSTRAK.....	xiii
ABSTRACT.....	xiv
CHAPTER 1	1
INTRODUCTION	1
1.1 Background of Study.....	1
1.2 Problem Statement	3
1.3 Aim of study	4
1.4 Research Objectives	4
1.5 Significance of Study	4
CHAPTER 2	5
LITERATURE REVIEW	5
2.1 SPECT/CT.....	5
2.2 SPECT/CT Quantification.....	6
2.2.1 Contrast.....	8

2.2.2 Signal to Noise Ratio (SNR)	8
2.2.3 Coefficient of Variation (COV)	8
2.2.4 Recovery Coefficient (RC)	9
2.3 SPECT/CT Reconstruction	9
2.3.1 CT based attenuation correction	10
2.4 Low Dose Computed Tomography	12
CHAPTER 3	15
MATERIALS AND METHODS	15
3.1 Materials	15
3.1.1 Discovery NM/CT 670 Pro SPECT/CT.....	15
3.1.2 NEMA 2012/IEC 2008 Phantom	16
3.1.3 ^{99m} Tc pertechnetate.....	17
3.1.4 25-cc syringe and Plastic tube.....	17
3.1.5 Well-type Ionization Chamber Dose calibrator: Atomlab TM 500.....	17
3.1.6 Xeleris Workstation.....	18
3.1.7 Q Metrix Software	18
3.2 Methodology	19
3.2.1 NEMA 2012/IEC 2008 phantom preparation	20
3.2.2 SPECT/CT Image Acquisition.....	23
3.2.3 SPECT/CT Image Reconstruction and Segmentation	25
3.2.4 Quantitative Analysis of Contrast, SNR, COV, RC	27

CHAPTER 4	30
RESULT AND DISCUSSION	30
4.1 SPECT/CT Acquisition	30
4.2 SPECT/CT Image Reconstruction	30
4.3 Quantitative Analysis	31
4.3.1 Contrast.....	31
4.3.2 Signal to Noise Ratio (SNR)	33
4.3.3 Coefficient of Variation (COV)	36
4.3.4 Recovery Coefficient (RC).....	38
4.4 Evaluation of CT dose.....	40
CHAPTER 5	43
CONCLUSION.....	43
5.1 Conclusion.....	43
5.2 Limitation of Study	44
5.3 Recommendation for Future Research.....	44
REFERENCES	45
APPENDICES	50
Appendix A	50
Appendix B	52
Appendix C	55

LIST OF TABLES

Table 3.1	Total activity required for each phantom preparation	22
Table 3.2	Imaging protocols of CT and SPECT	24
Table 3.3	OSEM reconstruction and Segmentation	27
Table 4.1	^{99m}Tc pre- and post-acquisition for TBR 10:1, 4:1 and to obtain calibration factor	30
Table 4.2	Results obtained from SPECT/CT Reconstruction	31

LIST OF FIGURES

Figure 3.1	GE Discovery NM/CT 670 Pro SPECT/CT	15
Figure 3.2	NEMA 2012/IEC 2008 phantom	16
Figure 3.3	Well-type Ionization Chamber Dose calibrator: Atomlab™ 500	17
Figure 3.4	Summary of the process of analysing quantification accuracy using different mAs and tumor background ratio	20
Figure 3.5	Preparation of NEMA phantom with ^{99m} Tc	23
Figure 3.6	The arrangement of the phantom for image acquisition	24
Figure 3.7	The coronal, sagittal and transaxial view of images	25
Figure 3.8	The contouring and segmentation process	26
Figure 4.1	The relationship contrast at different mAs for TBR 10:1	32
Figure 4.2	The relationship contrast at different mAs for TBR 4:1	32
Figure 4.3	The relationship between signal to noise ratio at different mAs for TBR 10:1	34
Figure 4.4	The relationship between signal to noise ratio at different mAs for TBR 4:1	34
Figure 4.5	The relationship between coefficient of variation at different mAs for TBR 10:1	36
Figure 4.6	The relationship between coefficient of variation at different mAs for TBR 4:1	37
Figure 4.7	Recovery Coefficient at various current for TBR 10:1	38
Figure 4.8	Recovery Coefficient at various current for TBR 4:1	39
Figure 4.9	The association between the current and CT dose index-volume	40
Figure 4.10	The association between the current and dose length product	41

LIST OF SYMBOLS

%	Percentage
A_0	Initial Activity
$T_{1/2}$	Half life
^{99m}Tc	Technetium-99m
A	Activity of radionuclide
kBq	Kilobecquerel
kVp	Kilovolt peak
MBq	Megabecquerel
mCi	Millicurie
ml	Millilitre
N	Mean Count
S	Standard Deviation
t	Time of Acquisition
TcO ₄ ⁻	Technetate(VII) ion
vol	Volume
λ	Decay constant

LIST OF ABBREVIATIONS

EANM	European Association of Nuclear Medicine
ROI	Region of Interest
3D	3-Dimensional
ALARA	As Low As Reasonably Achievable
COV	Coefficient of variation
CT	Computed Tomography
GE	General Electric
HUSM	Hospital University Sains Malaysia
mA	Milliampere
mAs	Milliampere-second
NEMA	National Electrical Manufacturers Association
CF	Calibration Factor
NM	Nuclear Medicine
OSEM	Ordered Subset Expectation Maximisation
PET	Positron Emission Tomography
RC	Recovery coefficient
SNR	Signal to Noise Ratio
SPECT	Single Photon Emission Computed Tomography
cps	Count per second
MRI	Magnetic Resonance imaging
TBR	Tumor to background ratio
VOI	Volume of Interest

AC	Attenuation Correction
NC	Non-attenuation Correction
DLP	Dose Length Product
CTDI	Computed Tomography Dose Index
ceCT	contrast-enhanced Computed Tomography
LDCT	Low Dose Computed Tomography

KESAN PEMBETULAN ATENUASI BERASASKAN CT TERHADAP KETEPATAN KUANTIFIKASI ^{99m}Tc SPECT/CT

ABSTRAK

Kajian ini mengkaji kesan pengurangan dos tomografi berkomputer (CT) terhadap ketepatan kuantifikasi Technetium-99m (^{99m}Tc) Pancaran Foton Tunggal Tomografi Berkomputer / Tomografi Berkomputer (SPECT/CT). SPECT/CT yang menggabungkan pengimejan berfungsi dan anatomi, adalah penting untuk diagnosis dan perancangan rawatan yang tepat dalam perubatan nuklear. Tetapi untuk mengurangkan dedahan terhadap pesakit sambil mengekalkan kualiti imej, dos radiasi dalam imbasan CT mesti dikurangkan. Penyelidikan ini melihat bagaimana pelbagai tetapan arus CT (mA) memberi kesan kepada ketepatan pembetulan pengecilan foton dan kualiti imej keseluruhan ^{99m}Tc SPECT/CT. Kajian ini menggunakan sistem GE Discovery NM/CT 670 Pro SPECT/CT dan fantom NEMA 2012/IEC 2008 yang diisi dengan ^{99m}Tc . Nisbah tumor-ke-latar belakang (TBR) adalah 10:1 dan 4:1 masing-masing. Terdapat beberapa tetapan mA, iaitu 30, 60, 90, 100, dan 120 mAs yang diuji untuk melihat kesan terhadap kualiti imej dan ketepatan kuantifikasi. Pembinaan semula imej dan kuantifikasi dijalankan menggunakan *workstation Xeleris* dan perisian Q.Metrix. Untuk menilai kualiti imej, metrik utama seperti kontras, nisbah isyarat-ke-hingar (SNR) dan pekali variasi (COV) digunakan. Untuk analisis kuantitatif, pekali pemulihan (RC) digunakan. Keputusan menunjukkan bahawa dos CT yang rendah yang dicapai dengan mengurangkan arus tiub boleh menghasilkan kualiti imej yang mencukupi untuk kuantifikasi tepat dalam ^{99m}Tc SPECT/CT. Kajian ini menunjukkan bahawa prinsip ALARA (As Low As Reasonably Achievable) boleh digunakan untuk mengurangkan dedahan radiasi kepada pesakit tanpa menjejaskan ketepatan diagnostik. Penemuan ini adalah penting untuk amalan klinikal yang bertujuan untuk meningkatkan keselamatan pesakit dengan mengurangkan dos radiasi sambil memastikan pengimejan diagnostik yang tepat dan boleh dipercayai.

THE EFFECTS OF CT-BASED ATTENUATION CORRECTION ON THE ACCURACY OF ^{99m}Tc SPECT/CT QUANTIFICATION

ABSTRACT

This study focuses on how CT- based attenuation correction affects the precision of quantification using Technetium-99m (^{99m}Tc) single-photon emission computed tomography/computed tomography (SPECT/CT). Functional and anatomical imaging are combined in SPECT/CT in nuclear medicine which is essential for precise diagnosis and therapy planning. To reduce patient exposure while retaining the image quality, CT scan radiation doses must be lowered. Therefore, this study investigates how varying CT current (mA) affects ^{99m}Tc SPECT/CT image quality overall and photon attenuation correction accuracy. In terms of methodology, the study used NEMA 2012/IEC 2008 phantoms filled with ^{99m}Tc and the GE Discovery NM/CT 670 Pro SPECT/CT system, using tumor-to-background ratios (TBR) of 4:1 and 10:1. The effects of various mA levels (30, 60, 90, 100, and 120 mA) on quantification accuracy and image quality were investigated. Image quantification and reconstruction were made easier using the Q.Metrix software and the Xeleris workstation, respectively. To evaluate the quality of the images, important metrics like contrast, signal-to-noise ratio (SNR) and coefficient of variation (COV) were examined. Recovery coefficients (RC) were utilised for quantitative analysis. According to the findings, low-dose CT which is accomplished by reducing the tube current can generate images with sufficient quality for precise quantification in ^{99m}Tc SPECT/CT. The study supports the ALARA (As Low As Reasonably Achievable) principle by showing that radiation exposure to patients can be decreased without sacrificing diagnostic accuracy. The significance of these findings lies in their potential to improve patient safety by lowering radiation doses while maintaining accurate and trustworthy diagnostic imaging.

CHAPTER 1

INTRODUCTION

1.1 Background of Study

Each and every day, patients' lives are improved by nuclear imaging treatments, which aid in the identification, diagnosis, prognosis, management, and surveillance of illnesses. Nuclear medicine imaging promise to continue improving patient care with the advent of novel technologies and imaging agents, several of which are currently undergoing clinical studies.

In nuclear medicine, the radioactive source is injected into the body and molecular imaging procedures, where it becomes integrated in a particular tissue, organ, or process. An external device (such as a gamma camera, SPECT, or PET scanner) then detects this incorporation to provide information on organ function and cellular activity (Society of Nuclear Medicine and Molecular Imaging n.d.). Because they offer information on the structure and functionality of organs and tissues, PET/CT and SPECT/CT, which combine PET or SPECT with CT, have established themselves as standard diagnostic instruments (Society of Nuclear Medicine and Molecular Imaging n.d.).

Recent SPECT/CT scanners has made quantitative SPECT practical with the introduction of additional computational features like attenuation, scatter, resolution recovery, and dead time adjustments (Ferrando et al, 2018). There are few importances of quantitative SPECT. One of it is SPECT aids in providing a more accurate diagnosis (Smith, 2018). Other than that, Bailey et al, 201 states that SPECT also provides improved evaluation of radiation dosimetry and 3D biodistribution from radiopharmaceuticals. SPECT contributes valuable information on radiotracer uptake in target lesions and yields reliable, accurate, and strong tool for dosimetry and the characterization of bone diseases (Mutuleanu et al, 2023). In addition to that, it also helps in the optimization of acceptable damage to normal organs and maximal

absorbed dose to the cancer (Dickson et al, 2022). A variety of image-related factors (controllable and uncontrollable) affects the accuracy of quantitative SPECT. Dead time, lesion or organ size and shape, collimator, patient movement and organ location will cause negative bias in the quantitative values, which is an underestimation of the actual activity concentration. Meanwhile, acquisition time, matrix size and post-reconstruction smoothing filter will cause positive bias, which is an overestimation of the activity concentration (Dickson et al, 2022).

In order to compensate for photons that have been Compton-scattered or attenuated inside the body, methods that employ the density of the body's tissues which the CT data provide can be used to supplement the SPECT data. While CT data aren't necessary in every way to produce quantitative SPECT images, having readily available coregistered datasets for both SPECT and CT has undoubtedly made it easier to apply corrections for scattered and attenuated photons (Bailey et al., 2013). Regarding CT attenuation correction (AC), the CT image in iterative reconstruction is transformed into a map of attenuation coefficients for the appropriate radionuclide energy (Dickson et al, 2022). Even with substantial CT image noise, AC may be achieved with ultra-low-dose CT without sacrificing the quality of the SPECT image (Hulme et al, 2014). Some of the factors affecting accuracy of CT based attenuation correction is the patient and respiratory motion which causes misalignment (Carney et al, 2016). This misalignment results in errors in the registration of anatomical and functional data (Nordstrom et al, 2020). It is also affected by quality of CT scans, including noise and spatial resolution as well as the presence of artifacts and misregistration of SPECT or CT images (Bermudez et al, 2016).

Therefore, this study focuses on a technique that uses low-dose CT-based attenuation correction to improve the accuracy of ^{99m}Tc SPECT/CT measurement. Automatic tube current modulation is an example to provide images of diagnostic quality while lowering the dose given to the patient, adjusting the image quality, and adjusting the tube current (mA) with the

patient's size and anatomy (Ferrari et al, 2018). This method will minimise unnecessary radiation exposure while improving the quantity and quality of images.

1.2 Problem Statement

After a CT scan, the CT data is processed to create an attenuation map, which gives various tissues distinct attenuation coefficients. The SPECT images are then corrected using this map. Precise attenuation correction for SPECT/CT is essential for dependable quantitative analysis and appropriate interpretation of the results (Wu et al., 2013). But the radiation exposure from CT scans increases the risk about safety of the patient. There is a desire to lower dose as doctors and patients are more concerned about exposure to ionising and injected radiation doses during various medical imaging examinations. Reducing the dosage, however, may result in a poor-quality image or a longer examination (Fougere, 2016).

The choice of exposure parameters, especially high voltage and x-ray tube current (mA), greatly affects CT examination. A high level of these parameters increases staff and patient exposure, even though the diagnostic information remains the same. Reduced values of these parameters reduce exposure dose, but they may also give a CT scan result that is less beneficial for diagnosis (Tulik et al, 2020). The technological aspects of low dose CT include the optimisation of the pitch and slice thickness, automatic tube current modulation, decrease of the tube current and voltage, and iterative reconstructions (Gervaise et al., 2016).

This study focuses on lowering current (mA) that leads to low-dose CT scan which provides accurate quantification of images with adequate image quality. In specific, this study will explore if low-dose CT can preserve the integrity of attenuation maps, guaranteeing precise and trustworthy SPECT image correction without losing the quality of the diagnostic process and at the same time reduce the patient's exposure to radiation. The amount of milliamperes used is determined under influence of ALARA principle (As Low As Reasonably

Achievable) that aims to maintain diagnostic image quality while keeping radiation doses as low as reasonably attainable. The purpose of this study is to determine how different current (mA) in CT scan affects the SPECT/CT image quality using Tc-99m.

1.3 Aim of study

To assess the accuracy of ^{99m}Tc SPECT/CT quantification using low dose CT-based attenuation correction.

1.4 Research Objectives

1. To evaluate the impact of low-dose CT on ^{99m}Tc SPECT/CT image quality.
2. To assess the accuracy of the quantified ^{99m}Tc SPECT/CT reconstructed using low-dose CT-based attenuation correction.
3. To determine the association between the current and CT dose (DLP and CTDI) using SPECT/CT protocol.

1.5 Significance of Study

The aim of this study is to evaluate potential effects of CT-based attenuation correction on the accuracy of ^{99m}Tc SPECT/CT quantification. In medical imaging, radiation exposure from the procedure itself is the primary cause for concern. Thus, low-dose CT has gained more attention in an effort to lower the possible radiation risk. The potential for additional diagnostic and therapy applications rises with the implementation of precise quantitative SPECT/CT in certain therapeutic settings. A straightforward method for obtaining dependable and accurate quantitative results that will enable a successful clinical application is by using low dose CT. Since the CT dose can be manipulated by adjusting the tube current value, this study discuss about how this technique is used to produce accurate and clear images of various patient with different age and size without worrying about the radiation exposure towards the staff and patient.

CHAPTER 2

LITERATURE REVIEW

2.1 SPECT/CT

Since its development in the 1990s, single-photon emission computed tomography (SPECT) has been extensively utilised to diagnose a wide range of human ailments, including endocrine problems, heart diseases, and diseases of the central nervous system (Zhang et al., 2021). Over the past fifty years, the most significant advancements have been the creation of hybrid SPECT/CT systems, the application of attenuation correction, and the use of iterative reconstruction techniques. The preference for SPECT/CT devices over SPECT-only systems and the widespread use of the former have resulted from these improvements, solidifying SPECT/CT's position as the mainstay of nuclear medicine imaging (Ritt et al., 2014). Israel et al., 2019 states that recent patterns in the global market for new nuclear medical equipment sales attest to the sharp increase in SPECT/CT device installations. The inclusion of new data from the CT images to the SPECT reconstruction is another recent development that makes it possible to employ CT data for purposes other than image fusion and attenuation correction (Ritt et al., 2014).

Whenever single-photon-emitting tracers are used in testing for patients with malignancies, SPECT/CT is utilised in the majority of clinical settings. The availability of functional and structural data has demonstrated a significant effect on evaluation of cancer diagnostic potential (Israel et al., 2019). The ability to have co-registered anatomical and functional images displayed simultaneously in the same imaging frame is a key factor in the preference for SPECT/CT. As the patient table moves in a predefined manner during the acquisition of both SPECT and CT images, the associations between the voxels in the SPECT images and their CT images are typically well-defined (Ritt et al., 2014). A diagnostic CT

component is a feature of contemporary SPECT/CT machines. It is possible to improve the efficacy of this modality for evaluating tumours by incorporating a contrast-enhanced CT scan (ceCT) into the hybrid investigation. Furthermore, lytic metastases alone, including those found in lymphomas or renal cancer, as well as lesions that are mostly lytic in breast cancer, are challenging to identify using bone scintigraphy. The sensitivity of the research can be increased by detecting these lesions on the CT component of SPECT/CT (Israel et al., 2019).

2.2 SPECT/CT Quantification

SPECT has historically been regarded as a non-quantitative imaging technique (Ferrando et al., 2018). However, opportunities for quantification in SPECT imaging have been made possible by the development of hybrid SPECT/CT (single photon emission computed tomography with computed X-ray tomography) imaging equipment (Kupitz et al., 2021). The European Association of Nuclear Medicine (EANM) recently published a dedicated guideline on quantitative SPECT/CT. This guideline includes information on the potential applications of quantitative SPECT/CT, including providing trustworthy diagnosis, precise treatment response monitoring as well as prognosis and directing patient management choices, enhancing the reproducibility of theories, enabling the comparison of data between centres and facilitating (semi)automatic analysis. This is one of the most compelling aspects of the growing value of quantitative SPECT/CT (Dickson et al., 2023). The authors of the guideline note that bone lesion assessments are one of the primary uses of quantitative SPECT/CT.

Dickson et al., 2023 states that gamma cameras and SPECT/CT systems are frequently utilised for quantitative imaging in nuclear medicine. While still in the early years, quantitative SPECT/CT's uses are starting to become apparent. The rise in theragnostic and radionuclide therapy, along with the corresponding rise in customised treatment planning leads to the growing interest in quantitative SPECT/CT. Many nuclear medicine treatments that use

gamma-emitting therapeutic radionuclides have the special benefit of enabling SPECT/CT imaging to visualise and measure the radiopharmaceutical bio-distribution following administration (Dickson et al., 2023). With the currently employed (commercially accessible) reconstruction algorithm and hybrid SPECT/CT, quantitative SPECT imaging is conceivable. Consistent use of this technique in diagnosis may offer opportunities for quantification in standard clinical practice (Kupitz et al., 2021).

Additionally, imaging surrogates combined with quantitative SPECT/CT can be utilised to measure treatment response or disease progression, as well as to diagnose and select patients before radionuclide therapy. Opportunities in cardiac and neurological imaging are also increasing and applications in the quantification of bone tracers for orthopaedic and cancer applications are in development. Quantitative SPECT/CT makes it possible to comprehend the reason a particular patient subgroup does not benefit from radionuclide therapy while sufficiently addressing the target. Quantitative SPECT/CT has the potential to assist clinical development in determining the best course of action to be given to each patient when developing novel radionuclide medicines with a narrower therapeutic index (Dickson et al., 2023).

According to Dickson et al., 2023, for quantitative imaging, SPECT/CT imaging has long been considered as inferior to PET/CT. Nonetheless, significant advancements in SPECT/CT quantification have been made possible by innovations in hardware and software, such as the addition of measured CT-based attenuation correction, scatter correction, and partial volume effect correction. Using contemporary methods, quantification of SPECT/CT data can now be achieved in a process identical to PET/CT. But quantitative SPECT/CT has a lot of advantages over PET/CT, which could result in more diverse applications. An additional benefit of SPECT imaging is the ability to observe numerous physiological processes

simultaneously due to the radiopharmaceuticals' ability to be tagged with different radionuclides. Several equations can be used to quantitatively assess the SPECT/CT images.

2.2.1 Contrast

Image contrast, which is the difference in density between regions of the image (ROI) equivalent to different degrees of radioactive uptake in the patient, is a crucial parameter for image quality in SPECT. Image contrast is generally referred to the amount of the signal change of an object of interest, like a lesion (region of interest), to the signal level in the surrounding areas of the image (Tantawy et al., 2023).

2.2.2 Signal to Noise Ratio (SNR)

In nuclear medicine, the phrase "signal-to-noise ratio" (SNR) refers to a measurement of the true signal, or actual anatomy, in relation to noise. The signal-to-noise ratio, or SNR, measures how powerful the desired output signal is in relation to the background noise (Dinh et al., 2023). It describes the quality of a measurement. The principles relating to the signal-to-noise ratio in CT are similar to those in plain radiography. SNR's purpose is to distinguish the background and sphere region. It is difficult to obtain clean segmentation when the SNR is low. The sphere region is mixed in with the background in the low SNR segmentation result. The high-SNR image, on the other hand, offers precise segmentation with distinct edges. SNR is significant for this reason (Kumar, 2022).

2.2.3 Coefficient of Variation (COV)

Coefficient of variation, or COV refer to a statistical measure of how widely apart data points are from the mean in a data series. The ratio of the standard deviation to the mean is known as the coefficient of variation or COV (Higaki et al., 2020). Simply said, the standard deviation expresses the level to which the average value deviates from the mean. According to McKenzie et al., 2014, COV records the variation brought forth by the setup of the experiment.

Similar theory applies in radiology where the measure of statistics used to evaluate the variability of radiation dose delivery inside a phantom is called the coefficient of variation. It measures the extent to which radiation doses are dispersed or diffused over various areas or locations inside the phantom. Greater variability and possible inconsistency in dosage delivery are indicated by a higher coefficient of variation, whereas a lower coefficient of variation denotes a more uniform and consistent dose distribution (Insee, 2016). This measure is essential for assessing the precision and dependability of radiation therapy methods and apparatus. The degree of dispersion around the mean increases with increasing coefficient of variation. Smaller remaining values in relation to the expected value, the lower the COV. This points to a well-fitting model (Hayes, 2024).

2.2.4 Recovery Coefficient (RC)

Recovery coefficient (RC) is the ratio of perceived activity concentrations to genuine activity concentrations. The recovery coefficient (RC) in nuclear medicine imaging is defined as the radioactivity concentration obtained from tomographic imaging divided by the genuine activity concentration. The imaging system's restricted resolution causes the recovery-coefficient values near the centre of small objects to be less than 1 (Mohd Yusof et al., 2020).

2.3 SPECT/CT Reconstruction

Image acquisition and reconstruction are the fundamental components of precise clinical imaging, and their inventive development enhances diagnostic confidence. In comparison to 2D planar imaging, the latest SPECT/CT systems and the increased quantitative precision of 3D imaging provide a thorough and accurate reconstruction of the patient's anatomy as well as a distinct localization of the radiotracer uptake area. Tumor localization, treatment planning, and bio distribution studies of given radiopharmaceuticals are thus made possible by this. In clinical and scientific applications, the task of accurately quantifying

SPECT activity within a volume of interest (VOI) is crucial for evaluating the therapeutic response (Graffi et al., 2017).

Of the several iterative reconstruction techniques created to quicken the reconstruction pace, the Ordered Subset Expectation Maximisation (OSEM) algorithm is the most frequently applied. Numerous studies on the effectiveness of this method on radionuclides commonly employed in nuclear medicine for patient imaging and patient-specific dosimetry have been performed. OSEM reconstruction is crucial for two reasons. One is that even with a larger noise level in the reconstructed images, tiny spheres can be detected for a large number of updates. Lesion detectability also increases with object proximity to the detector. A few of the more studies are enhancements to quantification correction methods in SPECT, assessments of the precision of quantitative image reconstruction methods and resolution comparisons between SPECT/CT systems using machine-specific reconstruction algorithms (Graffi et al., 2017).

2.3.1 CT based attenuation correction

A technique called attenuation correction is used to eliminate soft tissue artefacts from SPECT images. Patients may have different attenuation artefacts; however, the most often corrected artefacts are those related to diaphragmatic attenuation in men and breast attenuation in women. The ultimate objective is to lessen the effects of attenuation to produce more consistent images that enable greater analysing assurance (Digirad, 2016). Based on Kupitz et al., 2021, attenuation correction and scatter correction are two specialised adjustments that have made it possible to achieve quantitative SPECT imaging due to advancements in SPECT image reconstruction. CT data from hybrid SPECT/CT imaging is used to accomplish advanced attenuation correction in SPECT reconstruction. CT data is obtained in the form of CTDI vol. Another important patient dosage descriptor in CT is the dose-length product (DLP). DLP can be calculated by multiplying the centimetres of coverage by the CTDIvol. The unit of DLP is mGy-cm. The average CTDIvol indicates the linear extent of the exposure to the patient, which

is described by DLP (Mayo-Smith et al., 2014). Therefore, if the scan length stays the same and the tube current increases, leading to a higher CTDIvol, the DLP will also increase. Dickson et al., 2023 also agrees that for quantitative SPECT/CT, attenuation correction based on CT data ought to be applied. The iterative reconstruction procedure should use the CT images as a map of attenuation coefficients for the appropriate radionuclide energy.

In some ways, the CT-based technology gives benefit in other aspects. For instance, CT images produce nearly noise-free attenuation maps because their statistical noise is far lower than that of radionuclide transmission images. Aside from that, the use of CT acquisitions spares the signal from being contaminated by SPECT or PET tracers and also saves money by removing the need to replace deteriorating transmission sources on a regular basis (Lee et al., 2016). The CT data add to the SPECT data by sharing details about the body tissue's densities can be applied to algorithms to compensate for attenuated photons or Compton-scattered inside the body (Bailey et al, 2013).

With hybrid SPECT-computed tomography (CT) scanners becoming more widely available, the potential application of nonuniform attenuation correction has also gained significant significance in recent years (Warwick et al., 2011). In order to adjust for attenuation during image reconstruction, the OSEM method with attenuation model was created. In specific, the CT attenuation data is converted to linear attenuation coefficients for the SPECT photon energy using bilinear or trilinear scaling methods. The CT-derived attenuation coefficients are modified to correspond to the energy peak of the SPECT emission. This produces an attenuation correction map, which is then used during SPECT image reconstruction to increase image quality and accuracy (Tavakoli et al., 2019). Warwick et al., 2011 claims that many factors that reduce image quality must be considered for accurate quantification of striatal SPECT imaging. These include photon dispersion, photon attenuation, collimator blurring, and the SPECT systems' low spatial resolution, which lowers count

densities through the partial volume effect. In order to account for lower counts derived from deeper brain areas, attenuation correction, or AC is used. According to a simulation research, striatal recovery is understated by roughly 90% in the absence of any adjustment and improves to roughly 50% in the presence of attenuation correction (AC) and scatter correction.

In a study, Saleki et al., 2019 analyse the effects of misregistration and attenuation correction (AC) versus non-attenuation correction (NC) images on each segment of the SPECT image for both quantitative and qualitative analysis. As a conclusion, the study demonstrated the significance of CT-based attenuation correction for cardiac pictures in hybrid SPECT/CT to enhance image quality. Significant variance was introduced by misalignment in the caudal, cephalad, ventral, and right directions, even with a change of just one pixel. Misregistration correction is recommended to be frequently applied in clinical myocardial perfusion imaging, even in cases of minor misalignment.

2.4 Low Dose Computed Tomography

The phrase "low dose CT" describes CT scans in which the image quality has been purposefully altered to lower the exposure dose while maintaining diagnostic effectiveness, as opposed to a "normal" or "standard" dose scan (Gervaise et al., 2016). Hybrid imaging, such as single photon emission computed tomography (SPECT) combined with low-dose CT (ldCT), has emerged as a new technique for semi-quantitative functional parameter analysis in the last ten years (Genseke et al., 2018).

This is because in nuclear medicine, dosage, image quality, and time are closely related (Tulik et al., 2020). With information essential to precise clinical diagnosis and patient care, quicker image acquisition times, and more detailed images that can include body parts, CT is widely regarded as one of the most significant medical advancements. However, compared to traditional diagnostic x-rays, CT provides far higher radiation doses (Kalra et al., 2015). Experts surmise that the primary cause of the roughly double rise in radiation exposure per

person has been the growing usage of medical imaging. From 15% in the early 1980s to 50% in the present, medical sources account for a larger part of the overall radiation exposure. In the United States, CT alone is responsible for 24% of all radiation exposure (Mathews et al., 2013), according to a March 2009 report published by the National Council on Radiation Protection and Measurements (Harvard medical school, 2021). A lot of nuclear medicine experts are interested in minimising the amount of ionising radiation that patients receive during SPECT/CT scans, with a focus on CT.

Montes et al., 2013 claims that compared to the effective dosage from the administration of radiopharmaceuticals, contribution of low-dose CT scans to the overall radiation dose for patients undergoing SPECT/CT tests is minimal. A low-dose CT scan is appropriate for attenuation correction and anatomic localization, as its lower dose justifies the scan. Previously, a study has been done by Su et al, 2019 by comparing delivered radiation dose between a low-dose and traditional CT scan protocols. From the research, it is concluded that compared to regular CT, the low-dose CT technique reduced radiation exposure by 90%.

Su et al., 2019 states that in addition to plain radiographs, intraoperative dynamic and such additional modalities, an increasing number of hip surgeons are using computed tomography (CT) to enable a more thorough assessment of the bony pathomorphology prior to surgery. They claim that with the use of contemporary three-dimensional (3D) reconstruction, physicians may more accurately conceptualise the morphology of the pelvis, acetabulum, and femur due to the comprehensive visual and quantitative information that a CT scan gives. However, hip preservation surgeons who treat children and young adults have legitimate concerns about the higher radiation exposure that comes with using CT data. These scans can now be done with a much lower radiation exposure due to recent technology advancements and improved guidelines. Adult and paediatric populations have both benefited from the effective application of low-dose CT imaging procedures for a range of diagnostic and surgical

uses. At the end of their study, Su et al., 2019 confirms that when compared to standard CT scans, a low-dose hip CT scan technique consistently produced a reduced radiation dosage. By following the low-dose CT procedure, radiation exposure was reduced by over 90% and variability was minimised, all the while preserving sufficient image quality for clinical evaluation and preoperative surgery planning.

In order to determine an appropriate range of CT acquisition parameters for low-dose protocols with respect to accurate SPECT attenuation correction (AC), Hulme et al., 2014 conduct a research that assesses the effects of computed tomography (CT) image noise and artefacts on quantitative single-photon emission computed-tomography (SPECT) imaging. At the end of their study, it is concluded that SPECT imaging is affected by noise and artefacts in CT images. Thus, when low-dose CT images are used for AC, a CT approach with higher kVp combined with lower mAs minimizes beam-hardening artefacts and maintain a reconstructed SPECT image accuracy of greater than 4%.

Gervaise et al., 2016 states that a standard abdomen and pelvic CT scan typically requires a dose of between 10 and 12 mSv while a low-dose scan of less than 3 mSv equals to a dose reduction of more than 75%. Additionally, Fougere, 2016 affirms that with ultra-low-dose CT, a patient's radiation exposure can be greatly decreased and an accurate attenuation correction can be made. This is especially crucial for paediatric patients and in cases when scheduled sequential imaging techniques (such mIBG-SPECT/CT) are involved. Moreover, image fusion and co-registration with other tests, including MR, can be effortlessly accomplished using the anatomical data of extremely low-dose CT, allowing for improved multimodality imaging.

CHAPTER 3

MATERIALS AND METHODS

3.1 Materials

This study is carried on at the department of Nuclear Medicine, Radiotherapy and Oncology, Hospital University Sains Malaysia (HUSM), Kubang Kerian, Kelantan. The materials and apparatus used is GE Discovery NM/CT 670 Pro SPECT/CT, NEMA 2012/IEC 2008 phantom, ^{99m}Tc pertechnetate source, 25-cc syringe and plastic tube to insert the source inside the phantom, well-type ionization chamber dose calibrator: AtomlabTM 500 to measure the activity of ^{99m}Tc , Xeleris workstation for image registration and reconstruction and finally Q Metrix software to yield the AC_{rec} of the spheres and background.

3.1.1 Discovery NM/CT 670 Pro SPECT/CT



Figure 3.1: GE Discovery NM/CT 670 Pro SPECT/CT

In HUSM, GE Discovery NM/CT 670 Pro SPECT/CT as shown in figure 3.1 was used for scanning. With hybrid imaging, Discovery NM/CT 670 Pro which specified to dual-head variable angle with 16-slice CT configuration was created to support in leading clinical discovery. This is a high-end SPECT/CT system that also has the extra versatility of a stand-alone diagnostic CT. It has advanced gantry robotics that enable simultaneous motions on

multiple axes, quick setup, and faster overall imaging time. It is also in charge of managing dose for both NM and CT imaging. A wide range of features are included to enhance patient comfort, lessen anxiety, and provide a better overall imaging experience. Compared to independent, traditional SPECT and CT scans, the Discovery NM/CT 670 can also reduce acquisition times, enhance dosage management and facilitate more convenient patient scheduling (MedWrench, n.d).

3.1.2 NEMA 2012/IEC 2008 Phantom



Figure 3.2: NEMA 2012/IEC 2008 phantom

Figure 3.2 shows the NEMA 2012/IEC 2008 phantom that was used during this study. It includes a lung insert, an insert with six different-sized spheres and a body phantom. It has the dimensions of 24.1 cm height x 30.5 cm width x 24.1 cm depth and a cylindrical insert dimension of 51 mm diameter x 180 mm length. It consists of six fillable spheres with inner diameter of 10 mm, 13 mm, 17 mm, 22 mm, 28 mm and 37 mm respectively. Volume of the empty space is 9.7 litre (Gamma Gurus, n.d). The National Electrical Manufacturers Association (NEMA) made modifications to it while adhering to the International Electrotechnical Commission's (IEC) guidelines (Capintec A Mirion Medical Company, 2021).

3.1.3 ^{99m}Tc pertechnetate

^{99m}Tc pertechnetate is a radiopharmaceutical diagnostic agent pertechnetate that made up of an oxyanion with the molecular formula TcO_4^- . It was inserted in the phantom as a radioactive agent. As pertechnetate distributes in the body similarly to iodine, it offers a wide range of applications in nuclear medicine. It has physical half-life of 6 hours and biological half-life of approximately 1 day. One of the technetium radiopharmaceuticals utilised in thyroid, colon, bladder, and stomach imaging is ^{99m}Tc pertechnetate ($\text{Na}^+ \text{}^{99m}\text{Tc} \text{O}_4^-$). There are eight oxidation states for technetium (^{99m}Tc), ranging from -1 to +7. Specifically, technetium's oxidation state in the pertechnetate anion ($^{99m}\text{TcO}_4^-$) is +7. The most stable technetium chemical species in aqueous solution is the pertechnetate anion (Radswiki et al, 2023).

3.1.4 25-cc syringe and Plastic tube

Since the NEMA phantom's six spheres have relatively small openings, ^{99m}Tc was inserted inside the phantom via a plastic tube that is connected to a 25-cc syringe.

3.1.5 Well-type Ionization Chamber Dose calibrator: Atomlab™ 500



Figure 3.3: Well-type Ionization Chamber Dose calibrator: Atomlab™ 500

(Else Solution. n.d)

Figure 3.3 shows the well-type ionization chamber dose calibrator: Atomlab™ 500 that is used for measuring the radioactivity of the source in this study. The Atomlab™ 500 offers

radionuclide activity measurements that are quick, precise, and easily compliant with even the toughest regulatory requirements. The components of the system include an auto ranging touch screen colour display, an electrometer with exceptional linearity, and a new low pressure ionisation chamber with a modified seal. (Dupharma A/S, n.d)

3.1.6 Xeleris Workstation

Practitioners in nuclear medicine (NM) or radiology uses the Xeleris software to display, process, archive, print, report and network NM data, including tomographic and planar scans. For clinical diagnostic purposes, the distribution of radionuclide tracers and anatomical structures in scanned body tissue can be shown, localised, and/or quantified using NM or PET data in conjunction with registered and/or fused CT or MRI scans, as well as physiological signals. DICOM-formatted patient data, images, curves, and reports are kept in a proprietary local database. When combined with the sophisticated applications that come with the Xeleris workstation, the results from the Discovery NM/CT 670 Pro are even more valuable (US Department of Veterans Affairs, n.d).

3.1.7 Q Metrix Software

GE Healthcare's latest software innovation in nuclear medicine that is Q.Metrix, enables quantitative precision in the field. Q.Metrix is an application that measures and reports standard uptake values in the target organ or lesion. It allows for multi-dimensional organ and lesion characterization and personalised, quantitative SPECT/CT results (Diagnostic and Interventional Cardiology, 2014).

3.2 Methodology

For this study, the SPECT/CT imaging was carried out utilising the GE Discovery NM/CT 670 Pro SPECT/CT and the NEMA 2012/IEC 2008 phantom filled with ^{99m}Tc . The process started with the preparation of the ^{99m}Tc source and NEMA phantom. Two tumor to background ratio (TBR) were considered in this study, specifically 10:1 and 4:1. To assess the effect of mAs on the accuracy of image, the system uses smart mAs which includes 30, 60, 90, 100, and 120 mAs.

The dosage report, which includes CTDIvol, scan time, and total DLP, were obtained upon the completion of the image acquisition procedure. Following that, Xeleris workstation was used for image registration and reconstruction using OSEM reconstruction algorithm. To obtain the activity concentration of the reconstructed images of the spheres and the background, the spheres with different volumes (37 mm, 28 mm, 22 mm, 17 mm, 13 mm, and 10 mm) were contoured and segmented using Q metrix software. In order to perform an analysis of the image quality, several counting statistics including the background standard deviation, mean counts of the spheres and background mean counts were utilised to compute the contrast, signal-to-noise ratio (SNR) and coefficient of variation (COV). Graphs were plotted using these values in order to analyse the differences between different currents with varying ratios of tumor background. Quantitative analysis was done using recovery coefficient (RC). Figure 3.4 summarizes the process of analysing quantification accuracy using different mAs and tumor background ratio.

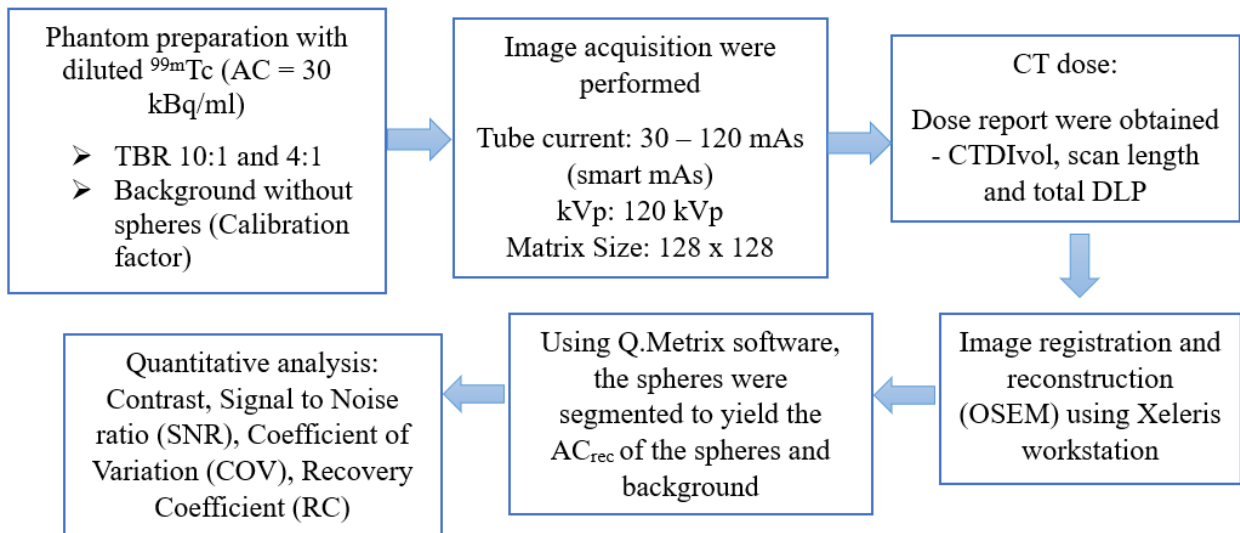


Figure 3.4: Summary of the process of analysing quantification accuracy using different mAs and tumor background ratio

3.2.1 NEMA 2012/IEC 2008 phantom preparation

The NEMA 2012/IEC 2008 phantom includes six different-sized spheres with volumes of 0.5 ml, 1.15 ml, 2.57 ml, 5.58 ml, 11.5 ml, 26.52 ml and a body phantom of 97 litre. At the centre of the phantom, a cylinder with an outer diameter of 51 mm filled with Styrofoam material represents the lung.

In this study, the sphere to background of 10:1 and 4:1 was considered, to represent the low and high TBR conditions of the tumor. The prepared activity concentration for background was 30 kBq/ml. As the total volume of the background of the phantom is equal to 9700 ml

hence, total amount of ^{99m}Tc required = $9700\text{ml} \times 30\text{kBq/ml}$

$$= 291\,000\text{kBq} \text{ (291MBq)}$$

The activity of the radioactive source is measured using Atomlab™ 500 Dose Calibrator. Considering the time gap taken between the phantom preparation and image acquisition, hence the prepared activity was corrected for this activity decay using Equation 3.1 and 3.2 (Britannica, 2024). Here is an example of the calculation, assuming time gap is 30 minutes.

$$A = A_0 e^{-\lambda t} \quad (3.1)$$

$$\lambda = \frac{\ln 2}{T_{1/2}} \quad (3.2)$$

Using Equation 1, as the $T_{1/2}$ of the ^{99m}Tc is 6 hours,

$$291 = A_0 e^{-\frac{\ln 2}{360 \text{ min}} (30 \text{ min})}$$

$$A_0 = 308.3 \text{ MBq} (8.32 \text{ mCi})$$

Thus, the total activity of ^{99m}Tc needed for background filling (9700 ml) is 308.3 MBq (8.32 mCi). Similar calculations were performed in determining the total activity of the ^{99m}Tc to be filled in the spheres. In this calculation, the activity concentration of the ^{99m}Tc was multiplied by the TBR considered for the respective spheres.

For example, for the 10:1 TBR, the activity concentration of the background is equal to 30 kBq (AC for background) $\times 10 = 300$ kBq/ml. Hence, the total amount of ^{99m}Tc of the six spheres = 48 ml $\times 300$ kBq/ml = 14 400 kBq (14.4 MBq). After eliminating the time gap of 30 minutes, the activity of ^{99m}Tc source for TBR 10:1 needed for six spheres is 15.26 MBq.

For the 4:1 TBR, the activity concentration of the background is equal to 30 kBq (AC for background) $\times 4 = 120$ kBq/ml. Hence, the total amount of ^{99m}Tc of the six spheres = 48 ml $\times 120$ kBq/ml = 5760 kBq (5.76 MBq). After eliminating the time gap of 30 minutes, the activity of ^{99m}Tc source for TBR 4:1 needed for six spheres is 6.103 MBq.

Due to the comparatively low predicted volume and activity of ^{99m}Tc for the spheres, ^{99m}Tc was diluted with 60ml of water. Thus, the total activity in 60 ml for 10:1 is equals to $\frac{15.26 \text{ MBq}}{48 \text{ ml}}$
 $\times 60 \text{ ml} = 19.07 \text{ MBq} (0.51 \text{ mCi})$

While for TBR 4:1 is equals to $\frac{6.103 \text{ MBq}}{48 \text{ ml}} \times 60 \text{ ml} = 7.63 \text{ MBq} (0.21 \text{ mCi})$.

The total activity required for each phantom preparation is summarized in Table 3.2.1.

TBR	AC (kBq/ml)	Total activity for 48 ml (MBq)		Total activity in 60 ml (MBq)
		At t = 0 min	At t = 30 min	
10:1	300	14.4	15.26	19.07
4:1	120	5.76	6.103	7.63

Table 3.1: Total activity required for each phantom preparation

The preparation of ^{99m}Tc is done as shown in Figure 3.5 (a). Regarding the background of the phantom, water was added into the phantom up to approximately 75% of its volume and then ^{99m}Tc is diluted in the background of phantom as shown in Figure 3.5 (b). Subsequently, using a fresh 25-cc syringe and plastic tube, the remaining volume is injected to the water to make sure there are no air bubbles in the background. This is due to the possibility that it may impede the acquisition and processing of images and result in a reduction in image quality. To make sure the activity is dispersed evenly inside the phantom, it was necessary to give it a gentle shake. The required ^{99m}Tc is prepared and is diluted inside 60ml of water as shown in Figure 3.5 (c). Using a syringe attached with a needle, 48 ml of the mixture were extracted from the diluted ^{99m}Tc (volume = 60 ml). Consequently, a 25-cc syringe with a plastic tubing connected is used to fill each of the spheres as shown in Figure 3.5 (d). Trained radio pharmacists follow established protocol to dilute ^{99m}Tc inside the phantom.



(a)



(b)



(c)



(d)

Figure 3.5: Preparation of NEMA phantom with ^{99m}Tc (a) The preparation of ^{99m}Tc (b) ^{99m}Tc diluted and filled inside the background of the phantom (c) The dilution of ^{99m}Tc inside 60ml of water (d) ^{99m}Tc was filled into the spheres using a 25-cc syringe with plastic tubing

The same preparation of ^{99m}Tc is done to obtain the calibration factor. However, the phantom is prepared without the presence of all six spheres to avoid any type of artifacts and distortions. As a result, the acquired calibration factor is accurate and reliable.

3.2.2 SPECT/CT Image Acquisition

The position of the NEMA 2012/IEC 2008 phantom for image acquisition was as indicated in the Figure 3.6.



Figure 3.6: The arrangement of the phantom for image acquisition

The imaging protocol for SPECT and CT is shown in the Table 3.2.

CT		
Voltage	120 kV	
Current	Smart mA (30, 60, 90, 100, 120)	
Matrix size	512×512	
SPECT		
Matrix Size	128×128	
Zoom	1	
Collimator	Low Energy High Resolution (LEHR)	
Scan mode (Step and shoot)	15 seconds	
Rotation	Total Angular Range	360°
	View Angle	6°
	Direction	Clockwise
	Arc per Detector	180
	Number of views	60

Table 3.2: Imaging protocols of CT and SPECT

In HUSM, Smart mAs is used. To maintain a user-selected noise level in the image, Smart mAs automatically modifies the tube-current along the angular and longitudinal directions based on patient size and attenuation level. In this study, the system automatically scans the phantom for all 5 mAs. The same acquisition steps with similar parameters are repeated to obtain the image of the phantom filled with TBR 4:1 of diluted ^{99m}Tc .